nature ecology & evolution

ARTICLES

https://doi.org/10.1038/s41559-018-0542-2

Native iron reduces CO_2 to intermediates and end-products of the acetyl-CoA pathway

Sreejith J. Varma[1,2], Kamila B. Muchowska[1,2], Paul Chatelain[1] and Joseph Moran[1*]

Autotrophic theories for the origin of life propose that CO_2 was the carbon source for primordial biosynthesis. Among the six known CO_2 fixation pathways in nature, the acetyl-CoA (AcCoA; or Wood–Ljungdahl) pathway is the most ancient, and relies on transition metals for catalysis. Modern microbes that use the AcCoA pathway typically fix CO_2 with electrons from H_2, which requires complex flavin-based electron bifurcation. This presents a paradox: how could primitive metabolic systems have fixed CO_2 before the origin of proteins? Here, we show that native transition metals (Fe^0, Ni^0 and Co^0) selectively reduce CO_2 to acetate and pyruvate—the intermediates and end-products of the AcCoA pathway—in near millimolar concentrations in water over hours to days using 1–40 bar CO_2 and at temperatures from 30 to 100 °C. Geochemical CO_2 fixation from native metals could have supplied critical C_2 and C_3 metabolites before the emergence of enzymes.

From the earliest stages of the transition from chemistry to biochemistry at the origin of life, synthetic pathways must have operated to build molecular complexity from simple starting materials. Life's fundamental need to build up carbon-based molecules has understandably orientated research on prebiotic chemistry towards high-energy C_1 and C_2 compounds such as HCN and formaldehyde, which react in ways that bear little resemblance to biosynthesis, often requiring ultraviolet light[1–3] (see also references within ref. [1]). However, as far as we can infer from extant biology, life has always built its biomass from CO_2. Could this attribute have extended back to prebiotic chemistry? Of the six known pathways of CO_2 fixation in nature[4,5], the acetyl-CoA (AcCoA; or Wood–Ljungdahl) pathway is the most ancient[6–8]. It reduces CO_2 to acetyl and then pyruvate—the ubiquitous C_2 and C_3 building blocks for life. Its enzymes and cofactors are replete with transition metals (Fe, Ni, Co, Mo or W) and, unlike the other five pathways, it is short, linear, exergonic and found in both bacteria and archaea, with the archaeal version being ATP-independent (Fig. 1)[9–12]. For all these reasons, the AcCoA pathway is often proposed to have prebiotic origins[13], although such a proposition faces some difficulties. Most modern microbes that run the AcCoA pathway fix CO_2 using electrons from H_2 gas, whose midpoint potential is not sufficient to generate the required highly reduced ferredoxin proteins in the absence of flavin-based electron bifurcation[14]. Therein lies a problem for autotrophic theories of the origin of life: how could CO_2 fixation have occurred before there were proteins to enable electron bifurcation? Many experimental attempts to address this question have bypassed the direct use of CO_2 altogether, focusing instead on its more reduced derivatives such as CO or formic acid[15,16]. However, clues from extant biology and the chemical literature suggest that native metals might warrant further experimental consideration as a prebiotic source of electrons for CO_2 fixation[17]. Even today, some bacteria that use the AcCoA pathway grow using native iron as the sole source of electrons[18,19]. We recently reported chemical experiments where many reactions of the reductive tricarboxylic acid (rTCA) cycle—another potentially prebiotic CO_2-fixing pathway—can be driven in sequence without enzymes using native iron as the source of electrons[20]. Meanwhile, freshly prepared native iron nanoparticles have been shown to reduce CO_2 to formate, with acetate formed as a minor product at 200 °C under 40 bar CO_2 pressure[21]. Before the emergence of electron-bifurcating enzymes, could native metals achieve reductive CO_2 fixation under conditions mild enough for a protometabolism?

Results

Anticipating a link between the role of metallic cofactors in extant microbial metabolism and in prebiotic chemistry[22–24], we set out to investigate whether the native forms of the metals involved in the reductive AcCoA pathway might promote C–C bond formation from CO_2 in water. Initially, we screened reactions of 1 mmol of Fe, Co, Ni, Mn, Mo and W powders (for specifications see Supplementary Table 1) in a 1 M KCl solution in deionized H_2O by heating to 100 °C under 35 bar CO_2 pressure for 16 h. The reaction mixtures were then treated with KOH to precipitate hydroxides, which were removed by centrifugation before analysis by ^{1}H NMR and gas chromatography mass spectrometry (GC-MS) (Supplementary Figs. 1–8). Quantification was achieved by comparison with a calibration curve prepared from authentic samples (Supplementary Fig. 9). To our surprise, all of these metals were found to promote the formation of acetate in up to 0.28 ± 0.01 mM concentrations, with considerable amounts of pyruvate observed in the cases of iron (0.03 ± 0.01 mM), nickel (0.02 ± 0.00 mM) and cobalt (0.01 ± 0.00 mM) (Fig. 2). Substantial quantities of formate (up to 2.3 ± 0.2 mM in the case of cobalt) and methanol (up to 0.39 ± 0.00 mM in the case of molybdenum) were also found in almost all cases. Control experiments in the absence of metal powders or in the absence of CO_2 did not produce detectable quantities of carbon fixation products (Supplementary Figs. 10 and 11).

In light of iron's position as the most Earth-abundant metal (predominantly as Fe^0 in the Earth's core and Fe^{2+}/Fe^{3+} in the Earth's mantle and crust)[25], we elected to study Fe-mediated CO_2 fixation in more detail by evaluating the influence of temperature, pressure, time, pH, salt identity and salt concentration on the reaction outcome. First, we studied the effect of temperature over the range 30–150 °C under typical conditions (35 bar CO_2, unbuffered 1 M KCl solution in deionized H_2O, 16 h) (Fig. 3a; see also

[1]Institute of Supramolecular Science and Engineering (UMR 7006), University of Strasbourg, National Center for Scientific Research , Strasbourg, France. [2]These authors contributed equally: Sreejith J. Varma and Kamila B. Muchowska. *e-mail: moran@unistra.fr

© 2018 Macmillan Publishers Limited, part of Springer Nature. All rights reserved.

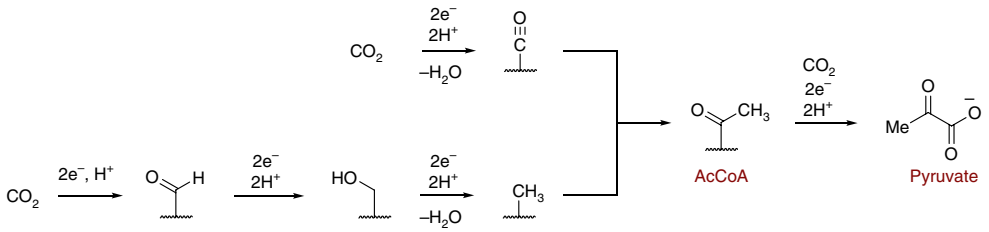

Fig. 1 | Mechanistic outline of the ATP-independent AcCoA pathway found in archaea. The reductive carboxylation of AcCoA to pyruvate is also found in the first step of the rTCA cycle. For clarity, organic and metallic cofactors are depicted as a squiggly horizontal line.

Supplementary Fig. 12 and Supplementary Table 2). At the lower end of the temperature range, acetate is the major product in solution, with pyruvate and formate produced in slightly smaller quantities. Increasing the reaction temperature to 100 °C results in the appearance of methanol among the other products. At 150 °C, pyruvate is no longer observed, presumably due to thermal decomposition. The reaction is robust to CO_2 pressure over the investigated range 1–40 atm at 30 °C, with acetate and pyruvate being the major products at lower pressures (Fig. 3b; see also Supplementary Fig. 13 and Supplementary Table 3). The reaction progress was monitored at different times under two representative sets of conditions. At 30 °C and 1 bar CO_2, acetate and pyruvate are the major products, with acetate reaching nearly 0.7 mM after 40 h before decreasing in concentration (Fig. 3c). At 100 °C and 35 bar CO_2, the initial build-up of formate is rapid, increasing to 7.2 ± 0.4 mM after 6 h before decreasing sharply as acetate and pyruvate begin to appear (Fig. 3d; see also Supplementary Fig. 14 and Supplementary Table 4). After 60 h, acetate and pyruvate reach maximal concentrations of 1.09 ± 0.00 mM and 0.11 ± 0.01 mM, respectively. Stopping the reaction at this time reveals that no Fe^0 visibly remains, although only ~1% of the available electrons from Fe^0 were channelled towards the described C_1–C_3 products in solution (assuming Fe^{2+} is the terminal product; see Supplementary Table 5), supporting previous observations that Fe^0 predominantly reacts to form hydrogen under these conditions[26]. By 85 h, the concentrations of all products in solution decrease, and ethanol is detected in the reaction mixtures for the first time (Supplementary Fig. 15). The disappearance of the Fe^0 'fuel' necessary to maintain the reaction in a steady state presumably causes the thermal decomposition of C_2 and C_3 products to outcompete their generation[27]. Neither changing the initial unbuffered pH nor swapping the K^+ electrolyte for other biologically relevant inorganic cations (Na^+, Mg^{2+} or Ca^{2+}) had significant influence on carbon fixation (Supplementary Figs. 16–26 and Supplementary Tables 6–17). However, the salt concentration had a small but significant effect, with a decrease in acetate and pyruvate yields by over 20% in the absence of KCl (Supplementary Fig. 27 and Supplementary Table 18).

Several additional experimental observations helped to gain insight into the mechanism of the reaction. First, in the absence of basic workup with KOH before NMR analysis, no C_1–C_3 carbon fixation products were observed in solution (Supplementary Fig. 29). Second, the introduction of formate, methanol or acetate into the reactor under typical reaction conditions did not result in their conversion to higher C_2 or C_3 products (Supplementary Fig. 30). Thus, formate, methanol and acetate, free in solution, do not appear to be intermediates in the reaction. Third, lactate—the product of pyruvate reduction—was never observed in any of our experiments, despite the fact that it is readily detected upon exposure of an aqueous pyruvate solution to native iron (Supplementary Fig. 30d). Fourth, Fe-mediated carbon fixation reactions performed with CO instead of CO_2 at 100 °C produced only tiny amounts of acetate and no detected pyruvate (Supplementary Fig. 31 and Supplementary Table 19). On the basis of these observations, we conclude that CO_2 fixation occurs on the surface of the metal and that its intermediates and end-products remain bound to the surface during the reaction. In light of this surface chemistry, the observed product distribution and the reaction's kinetic profile, we propose a plausible yet still largely hypothetical mechanism whereby the initial reduction of CO_2 occurs to generate surface-bound CO and formyl groups. Further reductions of the formyl group with expulsion of water lead to a surface-bound methyl group. Chain growth via migratory insertion of CO into the methyl group produces an acetyl species, which itself can undergo further migratory insertion of CO or reductive carboxylation with CO_2 to furnish a surface-bound pyruvyl or pyruvate species, respectively. The resistance of pyruvate or pyruvyl to reduction by Fe^0 may be rationalized by a diminished reactivity of the surface-bound species compared with pyruvate in solution. Basic workup at the end of the reaction with KOH is required to cleave the products from the surface to furnish formate, methanol, acetate or pyruvate in solution (Fig. 4). One possible interpretation of the kinetic profile observed in Fig. 3c is that the Fe surface becomes initially saturated with formyl and CO groups, with subsequent reactions of these groups producing acetyl and, eventually, pyruvyl groups[24]. Further detailed mechanistic study is required to distinguish between the possible intermediacy of surface-bound metal carboxylates and surface acyl metal species.

Besides the AcCoA pathway, another carbon fixation pathway that is often proposed to be ancient is the rTCA cycle[28] (also known

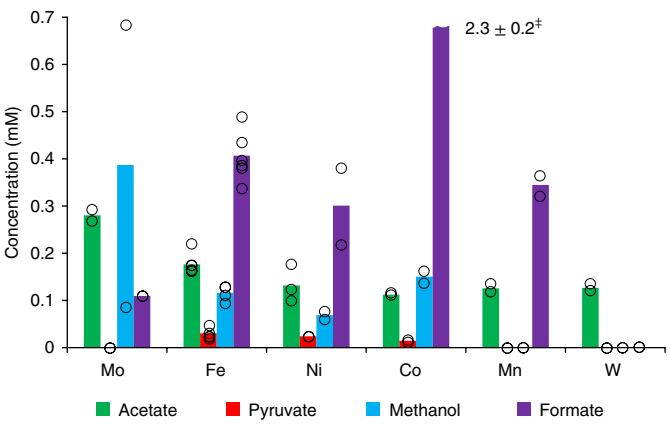

Fig. 2 | Carbon fixation by metals under hydrothermal conditions. Conditions were as follows: 100 °C, 35 bar CO_2, 1 M KCl in H_2O, pH = 7 (except for Mo, where the initial unbuffered pH was 2), 16 h (see Supplementary Information for experimental and analytical details, as well as error analysis). The bar chart shows the mean values of at least two independent runs, each of which is indicated by an open circle. ‡Formate concentrations for Co: 2.13 mM and 2.44 mM (the reported error corresponds to the mean absolute deviation).

© 2018 Macmillan Publishers Limited, part of Springer Nature. All rights reserved.

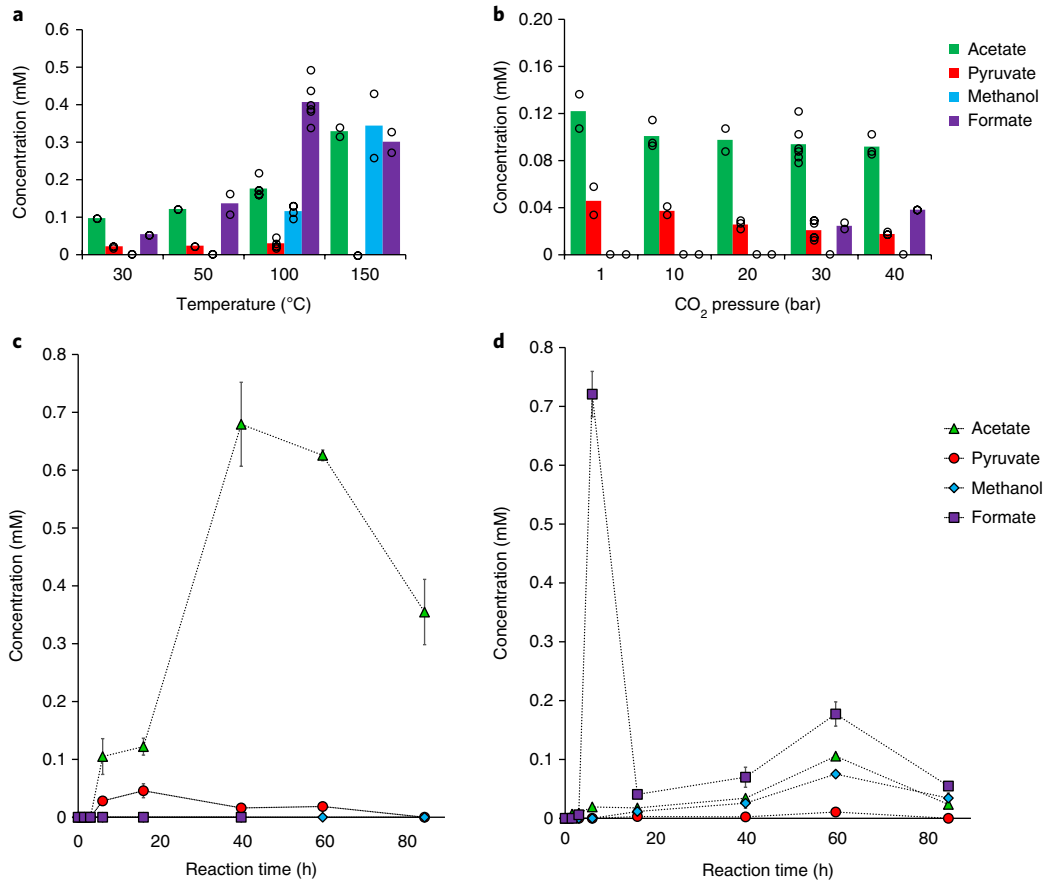

Fig. 3 | Effect of temperature, pressure and reaction time on iron-promoted CO_2 fixation in aqueous solution. a, Effect of temperature (35 bar CO_2, 16 h). **b**, Effect of CO_2 pressure (30 °C, 16 h). **c**, Reaction progress over time (30 °C, 1 bar CO_2). **d**, Reaction progress over time (100 °C, 35 bar CO_2). All reactions are 1 M Fe in 1 ml of a 1 M KCl solution. In **a** and **b**, the bar charts show mean values of at least two independent runs, each of which is indicated by an open circle. In **c** and **d**, error bars correspond to the mean absolute deviation from at least two independent runs. Lines connecting the data points do not represent a model fit.

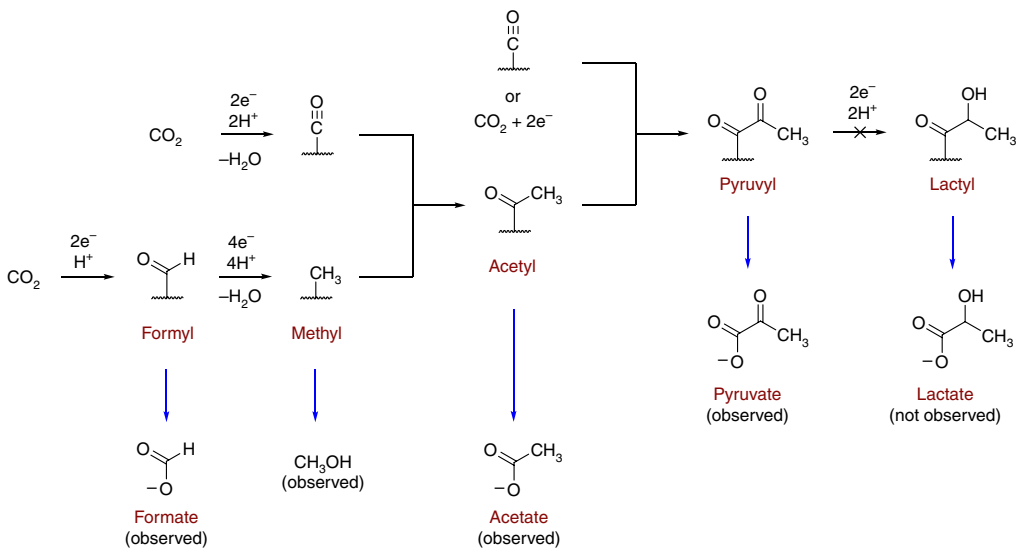

Fig. 4 | Plausible mechanism for carbon fixation on the surface of Fe^0 accounting for the detection of formate, methanol, acetate and pyruvate in aqueous solution upon hydrolysis with KOH. The depicted surface-bound acyl structures are deliberately ambiguous and may represent a surface-bound carboxylate or an acyl metal species. For clarity, organic and metallic cofactors are depicted as a squiggly horizontal line.

as the reverse Krebs, reductive citric acid or Arnon–Buchanan cycle; see Fig. 5), which contains five metabolites that collectively serve as the universal biosynthetic precursors for all of biochemistry[29–32]. A shorter, linear form of the rTCA cycle incorporating the first six steps (steps A–F), known as the 'horseshoe', also contains the same five crucial metabolites. We recently demonstrated that the

© 2018 Macmillan Publishers Limited, part of Springer Nature. All rights reserved.

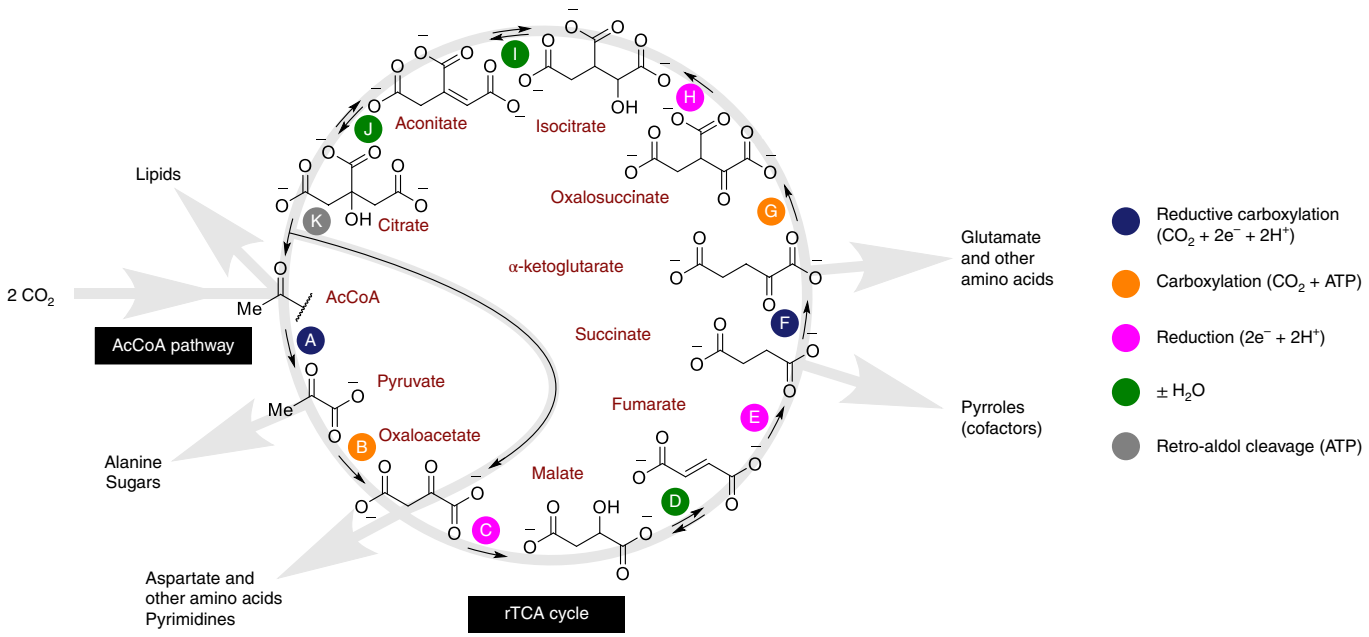

Fig. 5 | Hypothetical ancestral proto-anabolic network consisting of a hybrid of the AcCoA pathway and the rTCA cycle, showing the role of its intermediates as universal biosynthetic precursors. The 11 steps of the cycle (A–K) have been assigned colour-coded labels according to their chemical mechanisms.

combination of Fe^0, Zn^{2+} and Cr^{3+} under strongly acidic conditions (1 M HCl in H_2O) promotes 6 of the 11 steps of the rTCA cycle in the absence of enzymes, including the oxaloacetate-to-succinate sequence (steps C–E) and oxalosuccinate-to-citrate sequence (steps H–J)[20]. Since they share a common step (step A), it has been proposed that either the complete or 'horseshoe' forms of the rTCA cycle may have once been united with the AcCoA pathway in an ancestral, possibly prebiotic, carbon fixation network[13,24,33,34]. While these proposals provide strong explanatory power for the structure of extant metabolism, supporting chemical evidence is critically lacking. In light of the functional similarities between the CO_2 fixation reactions described in the current work and the AcCoA pathway, as well as the reliance of both chemistries on native iron, experiments were conducted to assess the mutual compatibility of the newly uncovered carbon fixation reaction with non-enzymatic reactions of the rTCA cycle. When oxaloacetate was heated for 16 h in the presence of Fe powder and Cr^{3+} at 140 °C under 35 bar of CO_2, an appreciable amount of succinate was formed, as evidenced by NMR and GC-MS (Supplementary Figs. 32 and 33). An analogous experiment carried out with in situ-generated oxalosuccinate (heated at 140 °C for 16 h under 35 bar of CO_2 in the presence of Fe powder and Cr^{3+}) resulted in the formation of citrate (detected by GC-MS; Supplementary Fig. 34). Although both of these reaction sequences are less selective under the mildly acidic conditions afforded by CO_2-saturated water than in 1 M HCl, they nonetheless suggest the potential compatibility of the carbon fixation conditions shown here with the non-enzymatic promotion of rTCA cycle reaction sequences. Lastly, the introduction of hydrazine into the otherwise identical Fe-rich conditions allowed for the non-enzymatic synthesis of the amino acid alanine from pyruvate (Supplementary Fig. 35)[20].

Discussion

We have shown that zero-valent forms of metals used by the cofactors and metalloenzymes of the AcCoA pathway fix CO_2 to selectively furnish the intermediates and end-products of this pathway in the absence of enzymes and in a manner robust to changes in temperature, pressure, salts and pH. Acetate is produced as the major C_2 product for all metals studied, whereas Fe^0, Ni^0 and Co^0 also produce pyruvate in up to ~0.1 mM concentrations, demonstrating that non-enzymatic C–C bond formation from CO_2 is possible in water under exceptionally mild conditions. The high selectivity of Fe^0 for the critical metabolites acetate and pyruvate at 30 °C and 1 atm CO_2 is remarkable considering the large number of C_2 and C_3 compounds derived from C, H and O that could possibly have been produced, suggesting that these compounds represent kinetic paths of least resistance for reductive organic synthesis from CO_2. Control and time-course experiments support a mechanism where CO_2 fixation occurs on the surface to produce surface-bound intermediates, notably reminiscent of some aspects of Wächtershäuser's initial theory of surface metabolism[29]. The temperature dependence and critical need to liberate surface-bound species with KOH before analysis may explain why pyruvate was not observed in previous studies on the reaction of CO_2 with Fe^0 (refs [21,26]). The CO_2 fixation reactions reported here are more geochemically plausible than the synthesis of activated acetate[15,35] from CO and CH_3SH, the low yielding and non-selective synthesis of pyruvate (0.07%) in formic acid at high temperature and high pressure (250 °C, 2,000 bar)[16], or using highly reducing (−1.1 V) electrochemistry on greigite electrodes[36]. Although native telluric iron deposits in the modern Earth's crust are relatively rare[37], native iron is produced in small amounts during serpentinization in the form of reduced FeNi minerals whose presence in surface samples indicates that they oxidize quite slowly[38,39]. Native iron is produced transiently in the mantle[40] and is the major component of the Earth's core. Iron meteorites, which constitute nearly 90% of known meteoritic mass, are mostly composed of native iron and its various alloys with nickel[41,42]. Thus, numerous plausible geological scenarios might be imagined in which Fe^0 or other reduced metals could have been continuously produced and consumed on the early Earth, in general agreement with the idea that metabolism originated to relieve pent-up redox gradients between the reduced iron that formed the early Earth's bulk and its comparatively oxidized CO_2-rich atmosphere and oceans[43]—a concept referred to as geobiotropy[44,45]. It may also

© 2018 Macmillan Publishers Limited, part of Springer Nature. All rights reserved.

help explain why pyruvate is found in some meteorites[46]. The Fe^0-promoted carbon fixation conditions are mutually compatible with Fe^0-promoted, non-enzymatic transformations of other supposedly ancient metabolic pathways, describing a set of reactions that play a synthetic role equivalent to the reductive AcCoA pathway, up to 7 of the 11 reactions of the rTCA cycle and amino acid synthesis. The observation that surface-bound pyruvate is not reduced to lactate in the presence of Fe^0—although not yet fully understood—opens up new mechanistic possibilities for how non-enzymatic anabolic reactions might be promoted selectively in the face of potential parasitic reactions[47]. The observed reactivity demonstrates an important parallel between plausible prebiotic chemistry and the ancient CO_2-fixing pathways used by primitive autotrophic life, supporting the hypothesis that geochemistry could have played an important role in the origin of life.

Methods

Analytical methods. ^{1}H NMR spectra were recorded on a Bruker Avance 300 (300 MHz) spectrometer at ambient temperature in a 6:1 H_2O:D_2O mixture as solvent, with sodium 3-(trimethylsilyl)-1-propanesulfonate (DSS-Na) as the internal standard (CH_3 peak at 0 ppm). Solvent suppression was achieved through excitation sculpting using the Bruker zgesgp pulse programme adjusted for the water resonance. In total, 32 scans were acquired for each sample. The relaxation delay was set to 87 s, with a time domain size of 32,768 and a sweep width of 4,789.27 Hz (11.963 ppm), to allow for quantitative measurements. Integration was performed using MestReNova version 6.0.2 software (http://mestrelab.com/download/mnova/). GC-MS analysis was performed on a GC System 7820A (G4320) using an Agilent High Resolution Gas Chromatography Column (PN, 19091S–433UI; HP, 5 ms; UI, 28 m × 0.250 mm; 0.25 µm; SN, USD 489634H). The system was connected to an MSD block 5977E (G7036A). Hydrogen (99.999% purity) was used as a carrier gas at a constant flow rate of 1.5 ml min^{-1}. The analysis was carried out in a splitless mode with a 1 µl injection volume, at an injection port temperature of 250 °C. The column was maintained at 60 °C for 1 min, then ramped at 30 °C min^{-1} to 310 °C with a 3 min hold, and the total running time was 12.33 min. The mass spectrometer was turned on after a 2 min solvent delay and operated in the electron ionization mode with a quadrupole temperature of 150 °C. Data were acquired in the full-scan mode (50–500 amu).

Product identification. Acetate, pyruvate, methanol, formate and lactate were identified based on the chemical shifts in the ^{1}H NMR compared with authentic samples using DSS-Na as the internal standard. Formate, acetate and pyruvate were additionally confirmed by GC-MS, where they were detected as their amides derived from *N*-methylphenylethylamine. Pyruvate was additionally confirmed by GC-MS. Pyruvate in the post-treatment sample was first reduced to lactate and converted to its ethyl ester (see below), since lactate esters have a better response than pyruvate esters[20]. See the Supplementary Information for more details regarding these procedures.

NMR sample preparation. Approximately 300 mg of solid KOH ($NaHS•xH_2O$ in the case of Mo-promoted reactions) was added to the reaction mixture to precipitate out any metal ions as their hydroxides (or sulphides in the case of Mo). This was mixed thoroughly. The resulting thick suspension was transferred to a 1.5 ml plastic microtube and centrifuged at 10,000 r.p.m. for 20 min. Then, 100 µl of 0.05 M solution of internal standard (DSS-Na in D_2O) was added to 600 µl of the supernatant. The resulting solution was analysed by NMR using the Bruker zgesgp pulse programme.

Yield determination and error analysis. Aqueous solutions of 700 µl potassium acetate, sodium methoxide, sodium pyruvate and sodium formate at different concentrations (0.71, 1.78, 3.57, 5.35, 7.14, 8.92 and 10.71 mM) were prepared by diluting their respective stock solutions (50 mM in Milli-Q water) with Milli-Q water to 600 µl and adding to each an aliquot of 100 µl of 50 mM solution of the standard compound (DSS-Na) in D_2O. Each of the samples was prepared in two replicas by two researchers and subjected to NMR spectroscopy (^{1}H, zgesgp water suppression, as described above). For each of these, three 32-scan spectra were acquired. The data from these 6 measurements for every concentration allowed us to obtain 7-point calibration plots for formate, methanol, acetate and pyruvate, correlating the substrate-to-standard ratios of peaks (8.45 ppm for formate, 3.34 ppm for methanol, 2.36 ppm for pyruvate and 2.08 ppm for acetate; 0 ppm for the methyl peak of the standard DSS-Na) with the product concentration (see Supplementary Fig. 9). The data points were subjected to least-squares fitting (intercept = 0), from which the calibration line equation was obtained. Detection thresholds were estimated for each analysed compound by integrating across the baseline in these regions of NMR spectra where no peaks were present, and were thus established to be 0.007 mM for acetate and pyruvate, 0.0016 mM for formate, and 0.0026 mM for methanol. We note that these values are much below the concentrations of acetate, pyruvate, methanol and formate detected in this study (see Supplementary Tables 2–19). Error bars on the calibration graphs correspond to ± s.d. for each data point. The yields of the CO_2 fixation experiments were calculated using the calibration coefficient corresponding to the slope of each calibration line. All yields of the CO_2 fixation experiments reported in this study are an average of at least two independent runs, with an error corresponding to ± mean absolute deviation (see Supplementary Information).

Metal-promoted CO_2-fixing reactions. To a 1.5 ml glass vial with a polytetrafluoroethylene (PTFE)-coated stir-bar, we added 1 mmol of each tested reagent (56 mg Fe, 58 mg Co, 58 mg Ni, 55 mg Mn, 96 mg Mo or 184 mg W and/or 58 mg NaCl and/or 75 mg KCl and/or 95 mg $MgCl_2$ and/or 111 mg $CaCl_2$) and 1 ml of Milli-Q water. To prevent cross-contamination, the vials were closed with caps bearing punctured PTFE septa. After placing the vials in a stainless steel 300 ml Parr pressure reactor, it was flushed with around 5 bar CO_2, pressurized to a final value of 35 bar CO_2 (unless otherwise noted) and stirred at the desired temperature (an external heating mantle was used where needed) for 16 h.

Assessment of compatibility of metal-promoted CO_2 fixation with rTCA cycle sequences. To a 1.5 ml glass vial with a PTFE-coated stir-bar, we added carboxylic acid substrate (oxaloacetic acid (0.03 mmol, 4 mg) or triethyl oxalosuccinate (0.03 mmol, ~8 µl)), Fe^0 powder (1.0 mmol, 56 mg), KCl (1.0 mmol, 75 mg) and $Cr_2(SO_4)_3·12H_2O$ (1 equiv., 0.030 mmol, 18 mg). This was followed by the addition of 1.0 ml of 0.24 M HCl in H_2O (2.0 µl conc. HCl in 1.0 ml Milli-Q water), which corresponds to an initial pH of ~0.6. To prevent cross-contamination, the vial was closed with a cap with a punctured PTFE septum. After placing the vial in a stainless-steel 300 ml Parr pressure reactor, it was flushed with around 5 bar CO_2, pressurized to a final value of 35 bar CO_2 and stirred at 140 °C (an external heating mantle was used) for 16 h.

Procedure for reductive amination under conditions for metal-promoted CO_2 fixation. To a 1.5 ml glass vial with a PTFE-coated stir-bar, we added sodium pyruvate (1 equiv., 0.03 mmol, 3 mg) in 1 ml Milli-Q water, hydrazine monohydrate (2 equiv., 0.06 mmol, ~3 µl) and KCl (1.0 mmol, 75 mg), followed by Fe^0 powder (1.0 mmol, 56 mg). To prevent cross-contamination, the vial was closed with a cap with a punctured PTFE septum. After placing the vial in a stainless-steel 300 ml Parr pressure reactor, it was flushed with around 5 bar CO_2, pressurized to a final value of 35 bar CO_2 and stirred at 140 °C (an external heating mantle was used) for 16 h.

Reporting Summary. Further information on experimental design is available in the Nature Research Reporting Summary linked to this article.

Data availability. The data that support the findings of this study are available in the Supplementary Information.

Received: 17 November 2017; Accepted: 19 March 2018;

References

1. Ruiz-Mirazo, K., Briones, C. & de la Escosura, A. Prebiotic systems chemistry: new perspectives for the origins of life. *Chem. Rev.* **114**, 285–366 (2014).
2. Peretó, J. Out of fuzzy chemistry: from prebiotic chemistry to metabolic networks. *Chem. Soc. Rev.* **41**, 5394–5403 (2012).
3. Sutherland, J. D. Studies on the origin of life—the end of the beginning. *Nat. Rev. Chem.* **1**, 0012 (2017).
4. Berg et al. Autotrophic carbon fixation in archaea. *Nat. Rev. Microbiol.* **8**, 447–460 (2010).
5. Hügler, M. & Sievert, S. M. Beyond the Calvin cycle: autotrophic carbon fixation in the ocean. *Annu. Rev. Mar. Sci.* **3**, 261–289 (2011).
6. Ljungdahl, L. G., Irion, E. & Wood, H. G. Total synthesis of acetate from CO_2. I. Co-methylcobyric acid and co-(methyl)-5-methoxy-benzimidizolycobamide as intermediates with *Clostridium thermoaceticum*. *Biochemistry* **4**, 2771–2779 (1965).
7. Fuchs, G. Alternative pathways of carbon dioxide fixation: insights into the early evolution of life? *Annu. Rev. Microbiol.* **65**, 631–658 (2011).
8. Weiss, M. C. et al. The physiology and habitat of the last universal common ancestor. *Nat. Microbiol.* **1**, 16116 (2016).
9. Can, M., Armstrong, F. A. & Ragsdale, S. W. Structure, function, and mechanism of the nickel metalloenzymes, CO dehydrogenase and acetyl-CoA synthase. *Chem. Rev.* **114**, 4149–4174 (2014).
10. Schwarz, G., Mendel, R. R. & Ribbe, M. W. Molybdenum cofactors, enzymes and pathways. *Nature* **460**, 839–847 (2009).
11. Schuchmann, K. & Müller, V. Autotrophy at the thermodynamic limit of life: a model for energy conservation in acetogenic bacteria. *Nat. Rev. Microbiol.* **12**, 809–821 (2014).
12. Furdui, C. & Ragsdale, S. W. The role of pyruvate ferredoxin oxidoreductase in pyruvate synthesis during autotrophic growth by the Wood–Ljungdahl pathway. *J. Biol. Chem.* **275**, 28494–28499 (2000).

© 2018 Macmillan Publishers Limited, part of Springer Nature. All rights reserved.

13. Martin, W. & Russell, M. J. On the origin of biochemistry at an alkaline hydrothermal vent. *Phil. Trans. R. Soc. B* **362**, 1887–1926 (2007).
14. Herrmann, G., Jayamani, E., Mai, G. & Buckel, W. Energy conservation via electron-transferring flavoprotein in anaerobic bacteria. *J. Bacteriol.* **190**, 784–791 (2008).
15. Huber, C. & Wächtershäuser, G. Activated acetic acid by carbon fixation on (Fe,Ni)S under primordial conditions. *Science* **276**, 245–247 (1997).
16. Cody, G. D. et al. Primordial carbonylated iron–sulfur compounds and the synthesis of pyruvate. *Science* **289**, 1337–1340 (2000).
17. Sousa, F. L., Preiner, M. & Martin, W. F. Native metals, electron bifurcation, and CO_2 reduction in early biochemical evolution. *Curr. Opin. Microbiol.* **43**, 77–83 (2018).
18. Kato, S., Yumoto, I. & Kamagata, Y. Isolation of acetogenic bacteria that induce biocorrosion by utilizing metallic iron as the sole electron donor. *Appl. Env. Microbiol.* **81**, 67–73 (2015).
19. Daniels, L., Belay, N., Rajagopal, B. S. & Weimer, P. J. Bacterial methanogenesis and growth from CO_2 with elemental iron as the sole source of electrons. *Science* **237**, 509–511 (1987).
20. Muchowska, K. et al. Metals promote sequences of the reverse Krebs cycle. *Nat. Ecol. Evol.* **1**, 1716–1721 (2017).
21. He, C., Tian, G., Liu, Z. & Feng, S. A mild hydrothermal route to fix carbon dioxide to simple carboxylic acids. *Org. Lett.* **12**, 649–651 (2010).
22. Sousa, F. & Martin, W. F. Biochemical fossils of the ancient transition from geoenergetics to bioenergetics in prokaryotic one carbon metabolism. *Biochim. Biophys. Acta* **1837**, 964–981 (2014).
23. Morowitz, H. J., Srinivasan, V. & Smith, E. Ligand field theory and the origin of life as an emergent feature of the periodic table of elements. *Biol. Bull.* **219**, 1–6 (2010).
24. Camprubi, E., Jordan, S. F., Vasiliadou, R. & Lane, N. Iron catalysis at the origin of life. *IUBMB Life* **69**, 373–381 (2017).
25. Moore, E. K., Jelen, B. I., Giovanelli, D., Raanan, H. & Falkowski, P. G. Metal availability and the expanding network of microbial metabolisms in the Archaean eon. *Nat. Geosci.* **10**, 629–636 (2017).
26. Guan, G. et al. Reduction of aqueous CO_2 at ambient temperature using zero-valent iron-based composites. *Green Chem.* **5**, 630–634 (2003).
27. Boekhoven, J., Hendriksen, W. E., Koper, G. J. M., Eelkema, R. & van Esch, J. H. Transient assembly of active materials fueled by a chemical reaction. *Science* **349**, 1075–1079 (2015).
28. Evans, M. C. W., Buchanan, B. B. & Arnon, D. I. A new ferredoxin-dependent carbon reduction cycle in a photosynthetic bacterium. *Proc. Natl Acad. Sci. USA* **55**, 928–934 (1966).
29. Wächtershäuser, G. Before enzymes and templates: theory of surface metabolism. *Microbiol. Rev.* **52**, 452–484 (1988).
30. Smith, E. & Morowitz, H. J. *The Origin and Nature of Life on Earth: The Emergence of the Fourth Geosphere* (Cambridge Univ. Press, Cambridge, 2016).
31. Morowitz, H. J., Kostelnik, J. D., Yang, J. & Cody, G. D. The origin of intermediary metabolism. *Proc. Natl Acad. Sci. USA* **97**, 7704–7708 (2000).
32. Smith, E. & Morowitz, H. J. Universality in intermediary metabolism. *Proc. Natl Acad. Sci. USA* **101**, 13168–13173 (2004).
33. Braakman, R. & Smith, E. The emergence and early evolution of biological carbon-fixation. *PLoS Comp. Biol.* **8**, e1002455 (2012).
34. Braakman, R. & Smith, E. The compositional and evolutionary logic of metabolism. *Phys. Biol.* **10**, 011001 (2013).
35. Chandru, K., Gilbert, A., Butch, C., Aono, M. & Cleaves, H. J. The abiotic chemistry of thiolated acetate derivatives and the origin of life. *Sci. Rep.* **6**, 29883 (2016).
36. Roldan, A. et al. Bio-inspired CO_2 conversion by iron sulfide catalysts under sustainable conditions. *Chem. Commun.* **51**, 7501–7504 (2015).
37. Klöck, W., Palme, H. & Tobschall, H. J. Trace elements in natural metallic iron from Disko Island, Greenland. *Contrib. Mineral. Petrol.* **93**, 273–282 (1986).
38. McCollom, T. M. Abiotic methane formation during experimental serpentinization of olivine. *Proc. Natl Acad. Sci. USA* **113**, 13965–13970 (2016).
39. Sleep, N. H., Meibom, A., Fridriksson, T, Coleman, R. G. & Bird, D. K. H_2-rich fluids from serpentinization: geochemical and biotic implications. *Proc. Natl Acad. Sci. USA* **101**, 12818–12823 (2004).
40. Frost, D. J. et al. Experimental evidence for the existence of iron-rich metal in the Earth's lower mantle. *Nature* **428**, 409–412 (2004).
41. Darling, D. J. *The Universal Book of Astronomy* 260 (Wiley, Hoboken, 2004).
42. Krot, A. N., Keil, K., Scott, E. R. D., Goodrich, C. A. & Weisberg, M. K. in *Treatise on Geochemistry* 2nd edn Vol. 1 (eds Holland, H. & Turekian, K.) 1–63 (Elsevier, Oxford, 2014).
43. Russell, M. J., Hall, A. J. & Mellersh, A. R. in *Natural and Laboratory Simulated Thermal Geochemical Processes* (ed. Ikan, R.) 325–388 (Springer, Dordrecht, 2003).
44. Bassez, M.-P. Water, air, earth and cosmic radiation. *Orig. Life Evol. Biosph.* **45**, 5–13 (2015).
45. Bassez, M.-P. Anoxic and oxic oxidation of rocks containing Fe(II) Mg-silicates and Fe(II)-monosulfides as source of Fe(III)-minerals and hydrogen. Geobiotropy. *Orig. Life Evol. Biosph.* **47**, 453–480 (2017).
46. Cooper, G., Reed, C., Nguyen, D., Carter, M. & Wang, Y. Detection and formation scenario of citric acid, pyruvic acid, and other possible metabolism precursors in carbonaceous meteorites. *Proc. Natl Acad. Sci. USA* **108**, 14015–14020 (2011).
47. Orgel, L. E. The implausibility of metabolic cycles on the prebiotic earth. *PLoS Biol.* **6**, e18 (2008).

Acknowledgements

This project has received funding from the European Research Council under the European Union's Horizon 2020 research and innovation programme (grant agreement 639170). Further funding was provided by a grant from LabEx 'Chemistry of Complex Systems'. L. Allouche, M. Coppe and B. Vincent are gratefully acknowledged for assistance with the NMR experiments. We thank E. Smith and W. F. Martin for critical readings of this manuscript.

Author contributions

J.M. supervised the research and the other authors performed the experiments. All authors contributed intellectually throughout the study. J.M. and K.B.M wrote the paper, and S.J.V. and K.B.M. assembled the Supplementary Information. Important preliminary experiments were carried out by P.C.

Competing interests

The authors declare no competing interests.

Additional information

Supplementary information is available for this paper at https://doi.org/10.1038/s41559-018-0542-2.

Reprints and permissions information is available at www.nature.com/reprints.

Correspondence and requests for materials should be addressed to J.M.

Publisher's note: Springer Nature remains neutral with regard to jurisdictional claims in published maps and institutional affiliations.

© 2018 Macmillan Publishers Limited, part of Springer Nature. All rights reserved.

nature research

Corresponding author(s): Joseph Moran (moran@unistra.fr)

☐ Initial submission ☐ Revised version ☒ Final submission

Life Sciences Reporting Summary

Nature Research wishes to improve the reproducibility of the work that we publish. This form is intended for publication with all accepted life science papers and provides structure for consistency and transparency in reporting. Every life science submission will use this form; some list items might not apply to an individual manuscript, but all fields must be completed for clarity.

For further information on the points included in this form, see Reporting Life Sciences Research. For further information on Nature Research policies, including our data availability policy, see Authors & Referees and the Editorial Policy Checklist.

Experimental design

1. Sample size

Describe how sample size was determined.

This is a purely chemical manuscript and there are no advanced statistics involved. It is standard practice to perform 2-3 repetitions of each reaction.

2. Data exclusions

Describe any data exclusions.

This does not apply since there is no advanced statistics (apart from above mentioned).

3. Replication

Describe whether the experimental findings were reliably reproduced.

Every chemical experiment in the main manuscript was reported as the average of at least two runs.

4. Randomization

Describe how samples/organisms/participants were allocated into experimental groups.

N/A

5. Blinding

Describe whether the investigators were blinded to group allocation during data collection and/or analysis.

N/A.

Note: all studies involving animals and/or human research participants must disclose whether blinding and randomization were used.

6. Statistical parameters

For all figures and tables that use statistical methods, confirm that the following items are present in relevant figure legends (or in the Methods section if additional space is needed).

n/a	Confirmed	
☐	☒	The exact sample size (*n*) for each experimental group/condition, given as a discrete number and unit of measurement (animals, litters, cultures, etc.)
☒	☐	A description of how samples were collected, noting whether measurements were taken from distinct samples or whether the same sample was measured repeatedly
☐	☒	A statement indicating how many times each experiment was replicated
☒	☐	The statistical test(s) used and whether they are one- or two-sided (note: only common tests should be described solely by name; more complex techniques should be described in the Methods section)
☐	☒	A description of any assumptions or corrections, such as an adjustment for multiple comparisons
☒	☐	The test results (e.g. *P* values) given as exact values whenever possible and with confidence intervals noted
☐	☒	A clear description of statistics including central tendency (e.g. median, mean) and variation (e.g. standard deviation, interquartile range)
☐	☒	Clearly defined error bars

See the web collection on statistics for biologists for further resources and guidance.

Software

Policy information about availability of computer code

7. Software

Describe the software used to analyze the data in this study.	MS Excel was used for numerical data handling and processing (basic statistics, charts, tables). NMR spectra were integrated in MestReNova v.6.0.2. GC-MS data were processed (peak-picking, scaling) by the Agilent MassHunter software.

For manuscripts utilizing custom algorithms or software that are central to the paper but not yet described in the published literature, software must be made available to editors and reviewers upon request. We strongly encourage code deposition in a community repository (e.g. GitHub). *Nature Methods* guidance for providing algorithms and software for publication provides further information on this topic.

Materials and reagents

Policy information about availability of materials

8. Materials availability

Indicate whether there are restrictions on availability of unique materials or if these materials are only available for distribution by a for-profit company.	All materials are available from standard commercial chemical vendors.

9. Antibodies

Describe the antibodies used and how they were validated for use in the system under study (i.e. assay and species).	No antibodies were used.

10. Eukaryotic cell lines

a. State the source of each eukaryotic cell line used.	No eukaryotic cell lines were used.
b. Describe the method of cell line authentication used.	No eukaryotic cell lines were used.
c. Report whether the cell lines were tested for mycoplasma contamination.	No eukaryotic cell lines were used.
d. If any of the cell lines used are listed in the database of commonly misidentified cell lines maintained by ICLAC, provide a scientific rationale for their use.	No commonly misidentified cell lines were used.

Animals and human research participants

Policy information about studies involving animals; when reporting animal research, follow the ARRIVE guidelines

11. Description of research animals

Provide details on animals and/or animal-derived materials used in the study.	No animals were used.

Policy information about studies involving human research participants

12. Description of human research participants

Describe the covariate-relevant population characteristics of the human research participants.	This study did not involve human research participants.